

C. S. Edwards · H. A. Kim · C. J. Budd

# An evaluative study on ESO and SIMP for optimising a cantilever tie-beam

Received: date / Revised: date

**Abstract** We examine both the Evolutionary Structural Optimisation (ESO) and Solid Isotropic Microstructure with Penalisation (SIMP) methodologies by investigating a cantilever tie-beam. Initially, both ESO and SIMP produce designs with higher objective function values relative to a previously published ‘intuitive’ design. However, after careful investigation of the numerical parameters such as the initial design domain and the mesh-size, both methods obtain designs which have lower objective function values relative to the intuitive design. Thus a clearer understanding for the numerical parameters and their influence on optimisation methods is achieved.

**Keywords** topology optimisation · evolutionary structural optimisation (ESO) · solid isotropic microstructure with penalisation (SIMP)

---

## 1 Introduction

Topology optimisation is a method for finding the optimal material distribution within a fixed design domain  $\Omega$ . An optimum can be defined by various objective functions such as minimum compliance or a fully stressed design. The design domain is usually discretised using finite elements with the existence of the elements being the design variable.

Inherent to many topology optimisation methods is a numerical instability which results in chequerboard pat-

terns. There has been much research into the chequerboard phenomenon including Díaz and Sigmund (1995) who find the stiffness of a chequerboard pattern to be higher and therefore favoured over its continuous equivalent. Also, Jog and Haber (1996) find chequerboard patterns to be a result of mixed finite element models where the existence of an element is piecewise constant whilst the displacement of an element is piecewise linear. There have been various methods developed for dealing with chequerboard patterns including the use of higher order elements (Jog and Haber 1996), perimeter constraints (Haber et al 1996) and filtering to smooth the sensitivity distribution (Sigmund 1994). A review of numerical instabilities and how to deal with them can be found in Sigmund and Petersson (1998).

Solving optimisation problems with discrete design variables is generally considered to be more difficult than with continuous design variables (Sigmund and Petersson 1998). Thus, a typical method used to solve topology optimisation problems is to relax the layout design variable by introducing intermediate states for an element that are between solid and void. This new layout design variable is analogous to the continuous density of the element. However, this density is somewhat artificial and a design with a continuous density distribution cannot be manufactured. Therefore, the intermediate densities are penalised using a power-law to give them low stiffness thus producing a near discrete solution. This approach is referred to as Solid Isotropic Microstructure with Penalisation (SIMP) (Bendsøe 1989; Rozvany and Zhou 1991, presented in 1990; Rozvany et al 1992; Bendsøe and Sigmund 2003).

Reitz (2001) has shown that there exists a discrete solution to the SIMP problem if a sufficiently high penalisation is used. The proof contains the following assumptions; there is only one constraint (volume), the objective function is continuously differentiable and its derivatives are negative and bounded and also that there exists a unique discrete solution. Subsequently, Martínez (2005) relaxes these assumptions by showing, for example, the solution does not necessarily need to be unique. How-

---

C. S. Edwards · H. A. Kim  
Department of Mechanical Engineering  
University of Bath  
Bath, BA2 7AY  
Tel.: +44(0)1225 383375  
E-mail: C.S.Edwards@bath.ac.uk,  
H.A.Kim@bath.ac.uk

C. J. Budd  
Department of Mathematical Sciences  
University of Bath  
Bath, BA2 7AY  
Tel.: +44(0)1225 386241  
E-mail: C.J.Budd@bath.ac.uk

ever, using high values of penalisation can result in local minima since the penalised design problem is not convex (Pettersson and Sigmund 1998). Thus continuation or homotopy methods are used to increase the likelihood of obtaining a global minimum (Allgower and Georg 1990).

An alternative topology optimisation method is Evolutionary Structural Optimisation (ESO) (Xie and Steven 1993, 1997). ESO slowly removes redundant material to evolve the structure to an optimum. Redundant material is characterised by low local sensitivity values, for example strain energy, calculated using finite element analysis (FEA).

Unlike SIMP, ESO was originally developed as a heuristic method derived from engineering intuition. The subsequent research efforts over the following decade demonstrated numerically that ESO generally finds an optimal solution (Xie and Steven 1997). Noting that the ESO solution agreed well with the Michell structure where the compliance - volume (C-V) product is minimum, Tanakanen (2002) recently proposed that this reflects the objective function of the ESO method. It was outlined that the strategy of removing elements with low strain energy is analogous to Sequential Linear Programming (SLP) and leads to a constant strain energy distribution, hence minimising the C-V product.

Zhou and Rozvany (2001) introduced a numerical example where ESO's strategy of removing the elements increased the total compliance by a factor of 10. This was because the element removal under consideration fundamentally changed the way the loads were transmitted and hence the structure evolved to a sub-optimal solution.

Inspired by such an interesting problem, the current paper further investigates the test problem of Zhou and Rozvany (2001). The aim of this paper is to compare the optimisation ability of SIMP and ESO by considering the effects of discretisation, penalisation and initial design.

In the following section we briefly outline the optimisation problem formulations for the SIMP and ESO strategies. §3 defines the test example used for this investigation. The influence of mesh density and the initial design domain is analysed for ESO and then SIMP in the subsequent sections, which is followed by the conclusions.

## 2 Problem formulations for the topology optimisation methods

### 2.1 The SIMP approach

The SIMP formulation is based on the continuous problem of minimising the total compliance  $C$  parameterised by a vector of coordinates  $\boldsymbol{\xi} \in \Omega$  with a volume constraint  $V_c$ ,

$$\left. \begin{array}{l} \min : C \\ \text{subject to : } V \leq V_c \end{array} \right\}. \quad (1)$$

In the finite element environment, a set of  $n$  elements over  $\boldsymbol{\xi} \in \Omega$  is used to represent a structure. The design variable  $x(\boldsymbol{\xi})$  is the presence of material which is discrete. This is relaxed such that it is continuous over  $(0, 1]$ . The intermediate values are penalised by a power-law (typically, power  $p \sim 3$ ) to steer the solution to a discrete topology.

The optimisation problem is constrained to satisfy the elastic equilibrium equation (2) for global stiffness matrix  $\mathbf{K}$  and load vector  $\mathbf{f}$ .

$$\mathbf{K}\mathbf{u} = \mathbf{f} \quad (2)$$

The element stiffness  $\mathbf{K}_i$  can be written in terms of  $\mathbf{x} = \{x_1, x_2, \dots, x_n\}$  as

$$\mathbf{K}_i = x_i^p \mathbf{K}_0, \quad (3)$$

where  $x_i \in (0, 1]$  and  $\mathbf{K}_0$  is the element stiffness constant with  $x_i = 1$ . Using the above notation for symmetric  $\mathbf{K}$ , the total compliance is written as

$$C_p(\mathbf{x}) = \mathbf{f}^T \mathbf{u} = \mathbf{u}^T \mathbf{K} \mathbf{u} = \sum_i x_i^p \mathbf{u}_i^T \mathbf{K}_0 \mathbf{u}_i. \quad (4)$$

The SIMP optimisation problem is thus defined as

$$\left. \begin{array}{l} \min_{\mathbf{x}} : C_p(\mathbf{x}) = \sum_{i=1}^n x_i^p \mathbf{u}_i^T \mathbf{K}_0 \mathbf{u}_i \\ \text{subject to : } V(\mathbf{x}) \leq V_c \\ \quad : \mathbf{0} < x(\boldsymbol{\xi})_{min} \leq x(\boldsymbol{\xi}) \leq \mathbf{1} \end{array} \right\}, \quad (5)$$

where  $x(\boldsymbol{\xi})_{min}$  is a vector of minimum densities to avoid singularities and  $V(\mathbf{x})$  is the current total material volume (Bendsøe and Sigmund 2003).

SIMP has a well defined objective function and the optimisation problem in (5) can be tackled using a variety of sophisticated algorithms such as the Method of Moving Asymptotes (MMA) algorithm (Svanberg 1987).

The penalisation of SIMP causes the design space to be non-convex and thus there may exist local minima. When high values of  $p$  are used, local minima are often produced rather than the global minimum. Thus a continuation method, like that described by Pettersson and Sigmund (1998), is used for such problems. We implement SIMP initially with a penalisation of  $p_{init} = 1$  until a solution has converged. The penalisation is then increased by 0.5 and the current solution is used as the new initial topology. This process is repeated until the penalisation value gives as discrete solution as possible but does not cause the stiffness matrix  $\mathbf{K}$  to be ill-conditioned.

We implement SIMP in this paper using the MMA algorithm in conjunction with the MATLAB (The Math Works, Inc. 2004) code in Sigmund (2001).

## 2.2 The ESO approach

ESO optimises a structure by slowly removing material which has the lowest sensitivity value, such as stress or strain energy  $U$  defined in (6), from the design domain. The sensitivity chosen reflects the objective function of the optimisation problem. It has been proposed that the removal of elements with the lowest strain energy leads to a design with a uniform strain energy distribution (Tanskanen 2002).

$$U_i = \frac{1}{2} \mathbf{u}_i^T \mathbf{K}_i \mathbf{u}_i. \quad (6)$$

Unlike SIMP, ESO treats the design variable  $x$  as a discrete variable which takes a value of either ‘1’ when an element is present or ‘0’ when completely removed. Thus the element stiffness  $\mathbf{K}_i$  for ESO, written in terms of the elemental design variable  $x_i$  is

$$\mathbf{K}_i = x_i \mathbf{K}_0, \quad (7)$$

where  $x_i \in \{0, 1\}$ .

An outline of the ESO algorithm can be summarised as follows:

1. An optimisation problem is defined by specifying the kinematic conditions and the initial design domain, appropriately discretised, in the FE environment.
2. FEA computes the displacement field and hence the strain energy of the given design.
3. The elements which satisfy (8) are removed,

$$U_i \leq RR \cdot U_{min} \quad (8)$$

where  $RR$  is the rejection ratio and  $U_{min}$  is the minimum elemental strain energy. The rejection ratio controls the optimisation rate and needs to be sufficiently small to do so. Thus  $RR$  is defined empirically and is problem dependent.

4. Steps 2 to 3 are repeated until all elements are removed or the stiffness matrix  $\mathbf{K}$  becomes singular. The latter case is what we usually see.
5. Examine the evolutionary history and select the design which has a locally minimum objective function value and/or desirable volume ratio. We henceforth refer to the local and global minimum of the iteration history for a single run as the S-history local and S-history single-run-global minimum respectively.

Tanskanen (2002) shows that removing elements with the lowest strain energy achieves a structure with a minimum compliance - volume product. Thus an appropriate objective function is the compliance - volume product  $S(\mathbf{x})$ . Using equations (2) and (7), compliance is defined as

$$C(\mathbf{x}) = \sum_i x_i \mathbf{u}_i^T \mathbf{K}_0 \mathbf{u}_i \quad (9)$$

Letting the volume of an element  $j$  be  $v_j$  and for symmetric  $\mathbf{K}$ ,  $S(\mathbf{x})$  is defined as

$$S(\mathbf{x}) = CV = \mathbf{u}^T \mathbf{K} \mathbf{u} V = \sum_i x_i \mathbf{u}_i^T \mathbf{K}_0 \mathbf{u}_i \sum_j x_j v_j. \quad (10)$$

Thus we can write the optimisation problem as (Tanskanen 2002):

$$\left. \begin{aligned} \min_{\mathbf{x}} : S(\mathbf{x}) &= \sum_i x_i \mathbf{u}_i^T \mathbf{K}_0 \mathbf{u}_i \sum_j x_j v_j \\ : x_i &\in \{0, 1\} \quad i = 1, 2, \dots, n. \end{aligned} \right\}. \quad (11)$$

The ESO algorithm as described does not stop once the objective function  $S(\mathbf{x})$  has reached a minimum, it continues to remove elements until either all elements have been removed or the stiffness matrix  $\mathbf{K}$  becomes singular. This further removal of elements may lead to S-history local minima with significantly smaller volume than the S-history single-run-global minimum.

One of the main differences in the formulations for ESO and SIMP is the volume. ESO reduces the volume to find the optimum topology solution, whereas SIMP finds the optimum topology solution to the given volume specified a priori. Thus to make a precise comparison of the results from ESO with those of SIMP we will consider the ESO objective function  $S(\mathbf{x})$  and constrain SIMP to the final volume of the ESO solutions. The results are also to be compared with those of Edwards et al (2006) where ESO was implemented using von Mises stress as opposed to strain energy and SIMP was implemented using the heuristic updating scheme of Bendsoe and Sigmund (2003).

We implement ESO in this paper using an INTEL® FORTRAN compiler with the MA57 multi-frontal linear solver (Rutherford Appleton Laboratory 2004). The results from the MA57 linear solver have been validated against MATLAB (The Math Works, Inc. 2004). MATLAB is then used to produce the graphical images.

## 2.3 Numerical instabilities and filtering

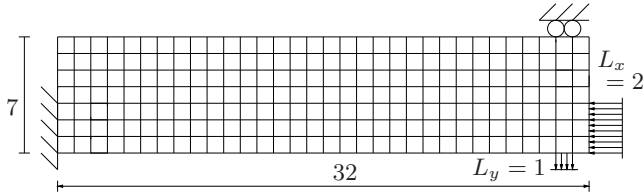
Topology optimisation can often exhibit an instability for which the resulting topology contains a checkerboard pattern of active and removed elements or of high and low density elements. It has been established that the appearance of these checkerboard patterns is a numerical instability and does not represent an optimal design (Sigmund 1994; Díaz and Sigmund 1995; Jog and Haber 1996; Kim et al 2000).



results of applying ESO to the revised test problems are presented.

#### 4.1 Investigation of ESO using a coarse mesh with a rectangular initial design domain

To investigate the effects of the initial design domain on the test problem, the initial design domain is modified to a rectangle containing the original problem and is shown in Figure 4.



**Fig. 4** Rectangular initial design domain encompassing original design domain with  $V(\mathbf{x}) = 224$ ,  $C(\mathbf{x}) = 283$  and  $S(\mathbf{x}) = 63430$

We apply ESO with the filtering technique of §2.3 to the ESO sensitivities by taking a weighted average of elemental strain energy. We use  $r_{min} = 1.05$  which is particularly small since the mesh is coarse. Experience has shown that a very small rejection ratio is also required to ensure slow material removal and therefore  $RR = 1.03$  is used. Using these optimisation parameters, an S-history single-run-global minimum is reached after 97 iterations.

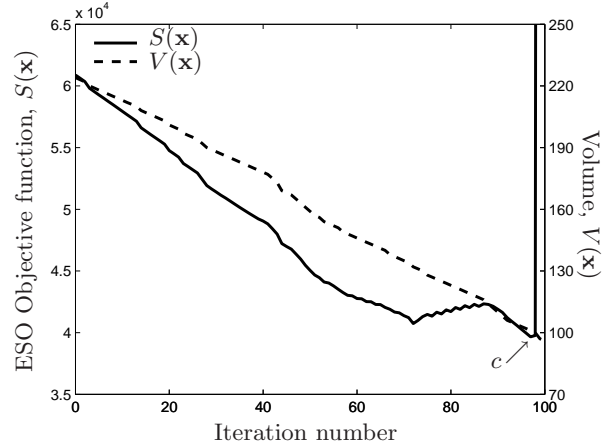
The material design  $\mathbf{x}$  of the S-history single-run-global minimum is illustrated in Figure 5 and has a volume of  $V(\mathbf{x}) = 101$ . The original initial design domain of Figure 1 has a similar volume to this S-history global solution with  $V(\mathbf{x}) = 100$ . However, the objective function for the S-history single-run-global minimum is  $S(\mathbf{x}) = 39997$  which is 3% higher than for the original initial design domain where  $S(\mathbf{x}) = 38986$ . The difference in  $S(\mathbf{x})$  is caused through the inability of ESO to replace previously removed elements if required.



**Fig. 5** S-history single-run-global minimum design of  $S(\mathbf{x})$  (c) by ESO for the rectangular initial design domain.  $V(\mathbf{x}) = 101$ ,  $C(\mathbf{x}) = 396$  and  $S(\mathbf{x}) = 39997$ . The compliance  $C(\mathbf{x})$  is calculated using the refined mesh of Figure 7

In comparison to the tie-beam solution of Figure 2, the S-history single-run-global minimum has lower  $S(\mathbf{x})$  and  $C(\mathbf{x}) = 396$  but higher  $V(\mathbf{x})$  since  $S(\mathbf{x}) = 44684$ ,  $C(\mathbf{x}) = 1117$  and  $V(\mathbf{x}) = 40$  for the tie-beam solution.

Thus the design of Figure 5 has a more efficient use of material, but more weight, compared to the tie-beam solution.



**Fig. 6** Iteration history for the ESO objective function when applied to a rectangular initial design domain. The sharp increase around ‘c’ represents the point where the vertical tie is detached.

Figure 6 shows the iteration history of the objective function  $S(\mathbf{x})$  and the volume  $V(\mathbf{x})$ . The S-history single-run-global minimum is achieved at ‘c’ (Figure 5). However, the volume continues to decrease since ESO does not have a stopping criterion and material continues to be removed. Thus the vertical tie becomes detached and the objective function increases significantly. The detachment of the vertical tie occurs only two iterations after the S-history single-run-global minimum (c) is achieved.

To understand why ESO cannot further reduce the volume of the test problem, we investigate the appropriateness of the given mesh size below.

#### 4.2 Investigation of mesh size

In order to understand why the ESO algorithm evolves the structure towards the cantilever beam, we return to the original initial design domain of Figure 1 and the optimality criterion of constant strain energy.

The tie-beam configuration primarily transmits the applied loads axially. Thus we simplify the configuration into a pin-jointed truss and ignore the negligible bending stress in region ‘B’ marked in Figure 1. The simplified system transmits the total horizontal load  $F_x$  and the total vertical load  $F_y$  completely to the horizontal beam and the vertical tie respectively.

Let  $A_x$  be the cross-sectional area to which  $F_x$  is applied and  $A_y$  be the cross-sectional area of the vertical tie which  $F_y$  is applied. Then the mean strain energy per element in the vertical tie is

$$\frac{F_y^2 d_y}{2A_y n_y E} \quad (14)$$

where  $d_y = 4$  is the length of the vertical tie and  $n_y$  is the number of elements in the vertical tie. Also, the horizontal beam has a mean strain energy per element of

$$\frac{F_x^2 d_x}{2A_x n_x E} \quad (15)$$

where  $d_x = 32$  is the length of the main beam and  $n_x$  is the number of elements in that beam. Thus for constant strain energy, we must have

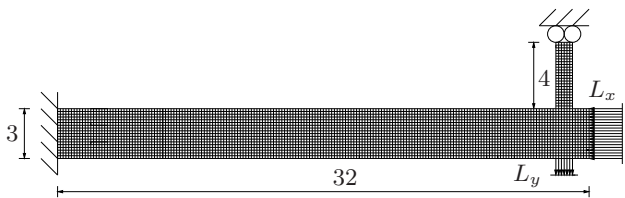
$$\frac{F_x^2 d_x}{2A_x n_x E} = \frac{F_y^2 d_y}{2A_y n_y E}. \quad (16)$$

The test problem has a horizontal load intensity of  $L_x = 2$  and a vertical load intensity of  $L_y = 1$ . These load intensities are measured in load per unit area where each element is of unit size. In the horizontal beam where the total cross-sectional area is 3 units, the total horizontal applied load is  $F_x = 6$ , and in the vertical tie the total vertical applied load is  $F_y = 1$ . Therefore the required cross-sectional area of the vertical tie for constant strain energy can be obtained as

$$\frac{6^2 \cdot 32}{2 \cdot 3 \cdot 96 \cdot 1} = \frac{1^2 \cdot 4}{2A_y \cdot 4 \cdot 1} \Rightarrow A_y = \frac{1}{4}. \quad (17)$$

The required element size for the vertical tie is  $1/4$  of the original element size. It can therefore be deduced that the vertical tie is eliminated in the early stages of optimisation because the vertical tie has a mesh which is too coarse to have constant strain energy. In order to compare the results those in Edwards et al (2006), the mesh is refined such that the element size is  $1/6$  of the original size.

#### 4.3 Investigation of ESO using a refined mesh with the original initial design domain



**Fig. 7** Original initial design domain with a refined mesh having  $V(\mathbf{x}) = 100$ ,  $C(\mathbf{x}) = 390$ ,  $S(\mathbf{x}) = 38986$

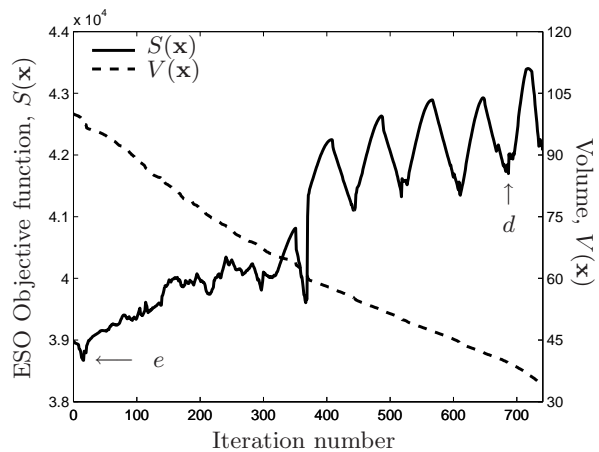
Applying the mesh refinement gives the initial design domain of Figure 7 which is the same as Figure 1 but with  $n = 3600$  plane stress elements. We optimise this test problem with the refined initial design domain via ESO again using  $RR = 1.03$ . However, the filter we apply is  $r_{min} = 2.5$  of the new element size. This is equivalent to  $r_{min} = 0.42$  of the original element size. The filter size is different to that used with the coarse mesh of the original initial design domain because an appropriate filter size for the new element size is smaller than the size of an original element.

To compare with the tie-beam solution, we select a design with a volume  $V(\mathbf{x}) \approx 40$ . Figure 8 presents a design with a volume of  $V(\mathbf{x}) = 39$ ,  $C(\mathbf{x}) = 1058$  and  $S(\mathbf{x}) = 41699$ . Comparing this design with the tie-beam solution of Figure 2, we find this S-history local minimum has the lower volume, compliance and thus volume - compliance product  $S(\mathbf{x})$ . We note that this design of Figure 8 exhibits a grillage-like structure at the beam-tie intersection and that the vertical tie remains.



**Fig. 8** Design for the S-history local minimum ( $d$ ) by ESO on a refined initial design domain with  $V(\mathbf{x}) = 39$ ,  $C(\mathbf{x}) = 1058$  and  $S(\mathbf{x}) = 41699$

Figure 9 shows the graph of the objective function  $S(\mathbf{x})$  and volume  $V(\mathbf{x})$ . The S-history local minimum of Figure 8 is marked ' $d$ ' at iteration 687. The graph clearly shows the volume decreases after the S-history global minimum has been achieved at ' $e$ ' and thus there exist other S-history local minima in between ' $d$ ' and ' $e$ '.



**Fig. 9** Iteration history of  $S(\mathbf{x})$ , for ESO applied to the refined initial design domain

The S-history single-run-global minimum occurs after only 16 iterations and is illustrated in figure 10. The compliance  $C(\mathbf{x}) = 392$  and the objective function  $S(\mathbf{x}) = 38671$ . However, the volume has only been reduced by 1% to  $V(\mathbf{x}) = 99$ . Thus, in terms of ESO, this design has the lowest  $S(\mathbf{x})$  of all designs so far, including the tie-beam solution of Figure 2.



**Fig. 10** Design for the S-history single-run-global minimum of  $S(\mathbf{x})$  ( $e$ ) by ESO on a refined initial design domain having  $V(\mathbf{x}) = 99$ ,  $C(\mathbf{x}) = 392$ ,  $S(\mathbf{x}) = 38671$

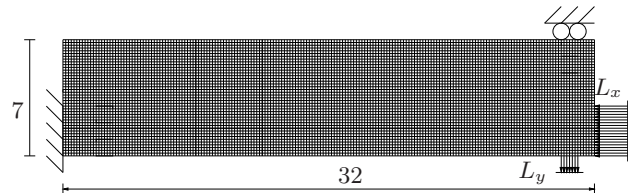
The two tie configuration design, illustrated in Figure 10, is favoured by ESO because there exists a local strain energy concentration at the re-entrant corners of the main beam where it meets the vertical tie at ‘ $F$ ’ for example. This local strain energy concentration increases the elemental strain energy along the boundary hence favouring the internal elements for removal. This pattern of element removal, determined by local concentrations, may be considered as a shortcoming of ESO since the severe strategy for the complete removal in ESO exacerbates the numerical issues at the sharp corners.

Edwards et al (2006) used von Mises stress as the sensitivity for ESO. An objective-history local minimum with volume  $V(\mathbf{x}) \approx 40$ , which has lower compliance than the tie-beam solution of Figure 2, was obtained. The topology of the objective-history local minimum also contained a grillage-like structure at the beam-tie interface. The objective-history single-run-global minimum obtained in Edwards et al (2006) also only had a 1% volume reduction and the vertical tie took the two tie configuration. Thus ESO produces consistent results whether von Mises stress or strain energy is used as the sensitivity.

#### 4.4 Investigation of ESO using the refined mesh with a rectangular initial design domain

We continue to investigate by applying ESO to a rectangular initial design domain with the finer mesh such that  $n = 6064$ , Figure 11.

As with the coarse mesh of Figure 4,  $S(\mathbf{x}) = 63430$  for the rectangular initial design domain, which is higher than  $S(\mathbf{x}) = 44684$  for the tie-beam solution of Figure 2. However, the previous design using a refined mesh (Figure 8) has an even lower  $S(\mathbf{x})$  (compared to the tie-beam solution of Figure 2). Thus we expect to achieve a design similar to that of Figure 8 rather than of the tie-beam solution of Figure 2.



**Fig. 11** Refined rectangular initial design domain encompassing original design,  $V(\mathbf{x}) = 224$ ,  $C(\mathbf{x}) = 283$  and  $S(\mathbf{x}) = 63430$

We apply ESO with  $RR = 1.03$  and with a filter of  $r_{min} = 2.5$  for the refined element size. An S-history local minimum of  $S(\mathbf{x})$  is produced and is illustrated in Figure 12. The volume for this design is  $V(\mathbf{x}) = 43$  and the compliance is  $C(\mathbf{x}) = 958$ . The objective of compliance and volume product is  $S(\mathbf{x}) = 41469$  which is marked ‘ $g$ ’ in Figure 13. The value of the objective function  $S(\mathbf{x})$  is slightly lower than for the design of Figure 8 using the original initial design domain.



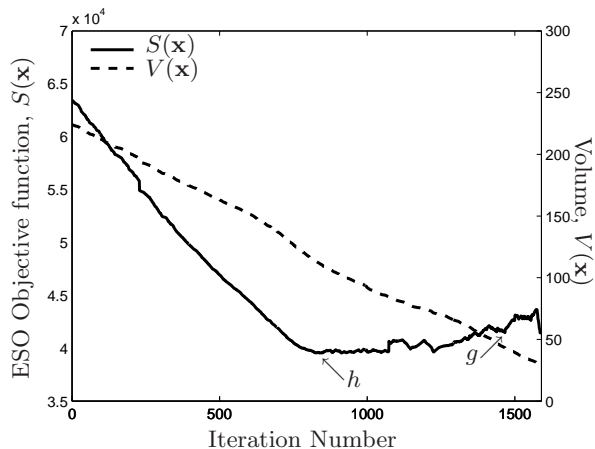
**Fig. 12** Material distribution for the S-history local minimum ( $g$ ) when ESO is applied to a refined rectangular initial design domain.  $V(\mathbf{x}) = 43$ ,  $C(\mathbf{x}) = 958$  and  $S(\mathbf{x}) = 41469$ .

Figure 13 shows the iteration history for  $S(\mathbf{x})$  and volume  $V(\mathbf{x})$ . The path of the objective function is smooth until ‘ $h$ ’ when the S-history single-run-global minimum is achieved. This design at ‘ $h$ ’ is similar to Figure 10 with a high volume of  $V(\mathbf{x}) = 111$ ,  $C(\mathbf{x}) = 355$  and  $S(\mathbf{x}) = 39543$ . The volume then continues to decrease as elements continue to be removed, thus producing the S-history local minimum at ‘ $g$ ’.

It is observed that designs of ESO are dependent on the mesh size and the numerical singularities caused by the severe complete removal strategy of ESO. If an appropriate mesh is used, then ESO obtains topological consistent solutions with a grillage-like configuration and is therefore not dependent on the initial design domain.

## 5 Application of SIMP

As a comparison to ESO, we now apply SIMP to both the original initial design domain and the rectangular initial design domain. SIMP is also implemented using these two design domains with finer computational meshes. SIMP is applied using the MMA algorithm and the continuation method, the initial penalisation of which is varied. In each case, SIMP is constrained to the final volume of the ESO calculations or to the tie-beam solution of Figure 2 where appropriate.

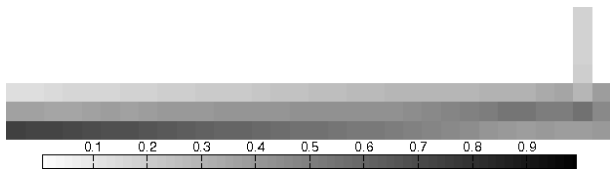


**Fig. 13** ESO iteration history where a refined rectangular initial design domain is used.

### 5.1 Investigation of SIMP using a coarse mesh with the original initial design domain

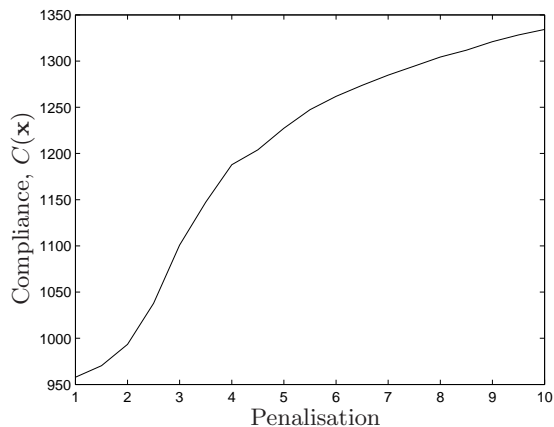
We begin this investigation by applying SIMP to the original coarse initial design domain of Figure 1 using the MMA algorithm and the continuation method described in §2.1. Throughout this section, the convergence of  $\mathbf{x}$  measured for iteration  $k$  is defined as  $\max |\mathbf{x}_k - \mathbf{x}_{k-1}| < 0.01$ . ESO did not find a solution to this original coarse design domain and therefore the volume constraint of SIMP is defined as  $V(\mathbf{x}) \leq 40$  so that the solution can be compared to the tie-beam solution of Figure 2. The filter is defined the same for ESO as  $r_{min} = 1.05$ .

The SIMP solution to the original test problem with a coarse mesh using  $p = 1$  is given in Figure 14 with  $C(\mathbf{x}) = 958$  and so  $S(\mathbf{x}) = 38373$ . However, this solution of Figure 14 is not discrete and thus has very low compliance  $C(\mathbf{x})$  and therefore  $S(\mathbf{x})$ . As the penalisation is increased, the solution becomes more discrete and hence the compliance also increases, as shown in Figure 15.



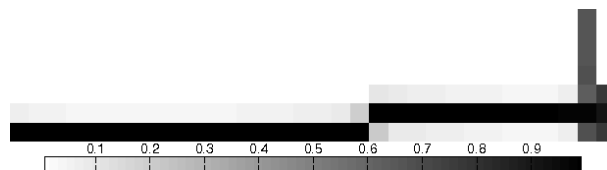
**Fig. 14** Solution obtained by SIMP with  $p = 1$ ,  $V(\mathbf{x}) = 40$ ,  $C(\mathbf{x}) = 958$  and  $S(\mathbf{x}) = 38373$ . The compliance  $C(\mathbf{x})$  is calculated using the refined mesh of Figure 7

If a penalisation of  $p > 10$  is used, the stiffness matrix  $\mathbf{K}$  becomes ill-conditioned. Thus we choose the solution for  $p = 10$  as a sufficiently discrete solution, which in this case is given in Figure 16 with  $C(\mathbf{x}) = 1334$  and so  $S(\mathbf{x}) = 53450$ . Unlike ESO, SIMP has produced a tie-beam-like solution with an equivalent volume to the tie-beam solution of Figure 2. However, the coarse repre-



**Fig. 15** Variation of compliance  $C(\mathbf{x})$  with penalisation  $p$  when implementing the continuation method to the original coarse initial design domain of Figure 1

sentation of the inclined main beam increases the compliance by 20% compared to the tie-beam solution of Figure 2.



**Fig. 16** Solution of SIMP with  $p = 10$ ,  $V(\mathbf{x}) = 40$ ,  $C(\mathbf{x}) = 1334$  and  $S(\mathbf{x}) = 53450$ . The compliance  $C(\mathbf{x})$  is calculated using the refined mesh of Figure 7

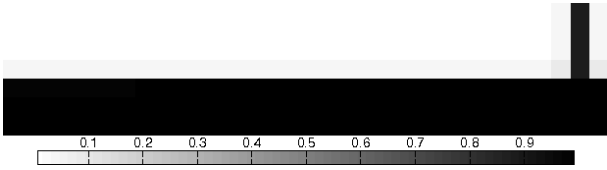
### 5.2 Investigation of SIMP using a coarse mesh with a rectangular initial design domain with

We apply SIMP to the rectangular initial design domain, Figure 4. To begin with we specify the volume constraint as  $V(\mathbf{x}) \leq 101$  to be consistent with the result obtained using ESO in Figure 5, and the filter as  $r_{min} = 1.05$ . The solution obtained is illustrated in Figure 17 with  $C(\mathbf{x}) = 385$  and  $S(\mathbf{x}) = 38926$  which is lower than for the original coarse design domain and the ESO solution of Figure 5.

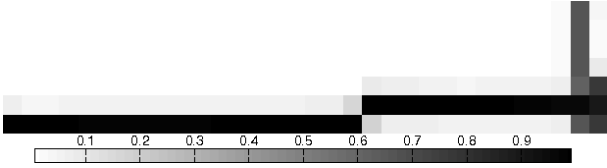
When we specify the volume constraint as  $V(\mathbf{x}) \leq 40$ , as it is for the tie-beam solution of Figure 2, and a filter of  $r_{min} = 1.05$ , application of SIMP leads to the minimum illustrated in Figure 18 with  $C(\mathbf{x}) = 1361$  and  $S(\mathbf{x}) = 54703$ .

Using a rectangular initial design domain when applying SIMP yields a similar design as with the original initial design domain. Edwards et al (2006) used a heuristic optimality criterion without continuation and





**Fig. 17** Solution obtained by SIMP with  $p = 10$ ,  $V(\mathbf{x}) = 101$ ,  $C(\mathbf{x}) = 385$  and  $S(\mathbf{x}) = 38926$ . The compliance  $C(\mathbf{x})$  is calculated using the refined mesh of Figure 7



**Fig. 18** SIMP solution using a rectangular initial design domain with  $p = 10$ ,  $V(\mathbf{x}) = 40$ ,  $C(\mathbf{x}) = 1361$  and  $S(\mathbf{x}) = 54703$ . The compliance  $C(\mathbf{x})$  is calculated using the refined mesh of Figure 7

also obtained similar inclined tie-beam solutions. However, it is observed that both  $C(\mathbf{x})$  and  $S(\mathbf{x})$  are consistently higher for the inclined SIMP solutions than for the tie-beam solution of Figure 2.

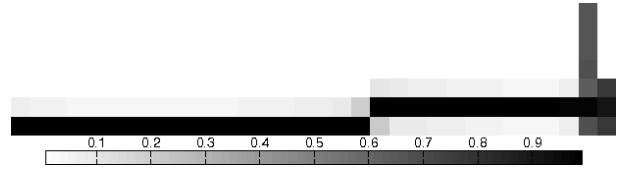
So far we have only found local solutions which suggest there exists multiple continuation paths to different local solutions (Allgower and Georg 1990). To find a solution with lower compliance than so far obtained with SIMP and the tie-beam solution of figure 2, we need to explore different continuation paths. Therefore we change the initial material layout by varying the initial penalisation  $p_{init}$  of the continuation method.

### 5.3 Investigation of initial penalisation of SIMP using the original coarse initial design domain

We now apply SIMP to the original coarse initial design domain of Figure 1 using the continuation method but with a different initial penalisation of  $p_{init} = 1.5$ . A discrete design is still required and so the upper bound of  $p_{upp} = 10$  remains. Also, the penalisation power remains to be increased reasonably slowly at increments of 0.5.

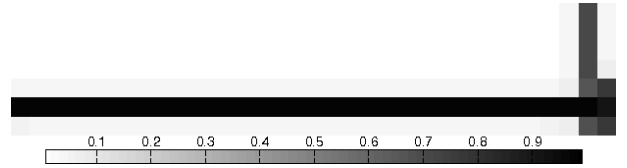
The revised continuation method is applied to the original initial design domain. The volume constraint remains as  $V(\mathbf{x}) \leq 40$ , as it is for the tie-beam solution of Figure 2, together with a filter of  $r_{min} = 1.05$ , which is sufficient to remove checkerboard patterns. This leads to the same continuation path and hence inclined tie-beam solution as in the previous section, Figure 19. This particular solution has  $C(\mathbf{x}) = 1334$  and  $S(\mathbf{x}) = 53450$ , which is exactly the same as that in Figure 16.

When the rectangular coarse initial design domain is used however, application of SIMP leads to a new minimum, Figure 20, which does have a horizontal main beam and a grey vertical tie.  $C(\mathbf{x}) = 1050$  and  $S(\mathbf{x}) = 42214$ ,



**Fig. 19** Minimum of SIMP for the coarse initial design domain using a revised initial penalisation of  $p_{init} = 1.5$ .  $p = 10$ ,  $V(\mathbf{x}) = 40$ ,  $C(\mathbf{x}) = 1334$  and  $S(\mathbf{x}) = 53450$ . The compliance  $C(\mathbf{x})$  is calculated using the refined mesh of Figure 7

which are significantly lower than the solid tie-beam solution of Figure 2 where  $C(\mathbf{x}) = 1117$  and  $S(\mathbf{x}) = 44684$ .



**Fig. 20** Minimum of SIMP for the coarse rectangular initial design domain using a revised initial penalisation of  $p_{init} = 1.5$ .  $p = 10$ ,  $V(\mathbf{x}) = 40$ ,  $C(\mathbf{x}) = 1050$  and  $S(\mathbf{x}) = 42214$ . The compliance  $C(\mathbf{x})$  is calculated using the refined mesh of Figure 7

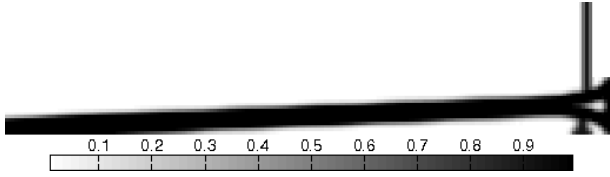
Further investigations have shown that when higher initial penalisation values are used, SIMP is destabilised and the solution reverts to that with an inclined main beam. In fact, only when the initial penalisation is in a small neighbourhood of  $p_{init} = 1.5$  do we obtain the horizontal main beam solution with lower compliance than the inclined tie-beam solutions and the tie-beam solution of Figure 2.

### 5.4 Investigation of SIMP using a refined mesh with the original initial design domain

SIMP is applied to the original initial design domain with refined mesh of Figure 7. The volume constraint is specified as  $V(\mathbf{x}) \leq 39$  to be consistent with the ESO solution in §4.3 and the filter is changed to  $r_{min} = 2.5$  for the refined element size, since the element size is now much smaller.

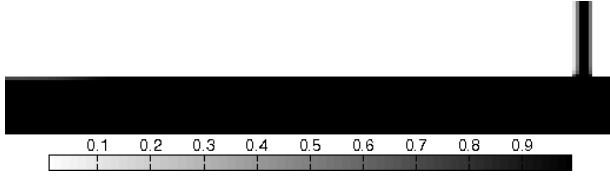
The solution, which contains an inclined main beam, is illustrated in Figure 21 with  $C(\mathbf{x}) = 1029$  and  $S(\mathbf{x}) = 40571$ .  $C(\mathbf{x})$  and  $S(\mathbf{x})$  are now lower than the tie-beam solution of Figure 2 and  $S(\mathbf{x})$  is within 3% of the equivalent design from ESO presented in Figure 8.

We now define the volume constraint to be the same as for the S-history single-run-global minimum of  $V(\mathbf{x}) \leq 99$ , which produces the solution illustrated in Figure 22. The compliance for this new solution is  $C(\mathbf{x}) = 397$  and  $S(\mathbf{x}) = 39197$ , which in both cases are slightly higher than for the ESO equivalent of Figure 10. Also, unlike the ESO equivalent solution,  $S(\mathbf{x})$  is higher for this SIMP



**Fig. 21** Minimum of SIMP using the refined initial design domain with  $p = 10$ ,  $V(\mathbf{x}) = 39$ ,  $C(\mathbf{x}) = 1029$  and  $S(\mathbf{x}) = 40571$

solution than it is for the original initial design domain of Figure 1.

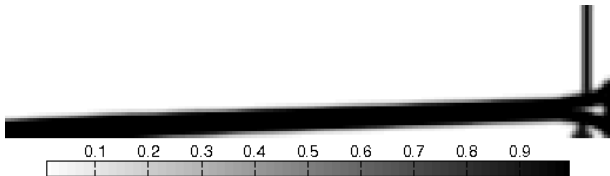


**Fig. 22** Minimum of SIMP using the refined initial design domain with  $p = 10$ ,  $V(\mathbf{x}) = 99$ ,  $C(\mathbf{x}) = 397$  and  $S(\mathbf{x}) = 39197$

The results thus far have shown that refining the mesh allows for SIMP to find smooth tie-beam-like designs with an inclined main beam when  $V(\mathbf{x}) \approx 40$  is specified. Edwards et al (2006) also obtained inclined tie-beam solutions with low compliance when the heuristic optimality criterion was used. We now change the design domain to be rectangular and refine the mesh.

### 5.5 Investigation of SIMP using a refined mesh with a rectangular initial design domain

SIMP is applied to the test problem with the rectangular initial design domain and a refined mesh, Figure 11. The filter of  $r_{min} = 2.5$  for the refined element size is used with the volume constraint of  $V(\mathbf{x}) \leq 43$ , which is the same as for the equivalent ESO solution of Figure 12. This leads to the smooth inclined design of Figure 23 with  $C(\mathbf{x}) = 935$  and  $S(\mathbf{x}) = 40996$ . The results are consistent with those of the original initial design domain with a fine mesh in §5.4.



**Fig. 23** Minimum of SIMP when applied to the refined test problem with a rectangular initial design domain.  $p = 10$ ,  $V(\mathbf{x}) = 43$ ,  $C(\mathbf{x}) = 935$  and  $S(\mathbf{x}) = 40996$

Results similar those of ESO are also obtained when SIMP is constrained to the higher volume of the S-history global optimum produced by ESO,  $V(\mathbf{x}) \leq 111$ . This solution has a compliance of  $C(\mathbf{x}) = 350$  and  $S(\mathbf{x}) = 39035$ . Therefore, SIMP also finds that the larger volume solutions have a better stiffness - volume ratio compared to the solutions with  $V(\mathbf{x}) \approx 40$  solutions.

Refining the mesh for either initial design domain, results in an inclined tie-beam solution when  $V(\mathbf{x}) \approx 40$  is specified. These smooth solutions then have lower compliance  $C(\mathbf{x})$  and  $S(\mathbf{x})$  compared to the tie-beam solution of Figure 2. They are also comparable to the results from ESO (§4.3 and §4.4). We note here that changing the initial penalisation of the continuation method as we did in §5.3 does not change the material layout of the solution. An inclined tie-beam solution is always achieved.

## 6 Conclusions












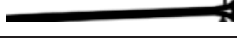

Topology optimisation methods of ESO and SIMP have been investigated using the tie-beam test problem introduced in Zhou and Rozvany (2001). ESO and SIMP were likely to encounter some difficulties since they were solving integer programming problems using heuristic algorithms based on local sensitivities. This investigation has identified some of the difficulties associated with the two methods and the reasons behind the said difficulties. A comprehensive summary of the results is given in Table 1.

ESO and SIMP solve different optimisation problems, however, their objective functions are both based on compliance and volume. SIMP solves for a continuous minimiser which has low compliance for a specified volume and produces a smooth solution.  $S(\mathbf{x})$  is the discrete objective function used with ESO and produces a number of minima representing a balance of compliance and volume. Given the numerical difficulties in solving such problems, both methods have been observed to perform well.

ESO failed to solve the test problem with the given coarse initial design domain. However, a simple analysis indicated that the mesh of the test problem was too coarse for further optimisation. Hence, due to the lack of termination criteria together with the severe complete element removal in the current ESO algorithm, non-optimal modification in a coarse mesh environment was inevitable. This non-convergent property of ESO needs to be addressed, perhaps by an appropriate element addition algorithm.

Upon mesh refinement or the use of an enlarged initial design domain, ESO was able to find consistent topological tie-beam solutions. These tie-beam solutions of ESO had reductions on both  $S(\mathbf{x})$  and  $C(\mathbf{x})$  when compared to the tie-beam solution in Zhou and Rozvany (2001). In fact, the solution with the lowest  $S(\mathbf{x})$  was produced by ESO.

**Table 1** A summary of all SIMP and ESO solutions

Optimisation method and parameter	Solution	$S(\mathbf{x})$	$C(\mathbf{x})$	$V(\mathbf{x})$
Intuitive tie-beam solution (Zhou and Rozvany 2001)	 (Figure 2)	44684	1117	40
SIMP solution, original $\Omega$	 (Figure 16)	53450	1334	40
SIMP solution, rectangular $\Omega$	 (Figure 18)	54706	1361	40
SIMP solution, original $\Omega$ , $p_{init} = 1.5$	 (Figure 19)	53450	1334	40
SIMP solution, rectangular $\Omega$ , $p_{init} = 1.5$	 (Figure 20)	42214	1050	40
ESO solution, rectangular $\Omega$	 (Figure 5)	39997	396	101
SIMP solution, rectangular $\Omega$	 (Figure 17)	38926	385	101
ESO solution, refined original $\Omega^1$	 (Figure 10)	38671	392	99
SIMP solution, refined original $\Omega$	 (Figure 22)	39197	397	99
ESO solution, refined original $\Omega$	 (Figure 8)	41699	1058	39
SIMP solution, refined original $\Omega^2$	 (Figure 21)	40571	1029	39
ESO solution, refined, rectangular $\Omega$	 (Figure 12)	41469	958	43
SIMP solution, refined, rectangular $\Omega$	 (Figure 23)	40996	935	43

<sup>1</sup> Minimum  $S(\mathbf{x})$  of all solutions<sup>2</sup> Minimum  $S(\mathbf{x})$  of all solutions with  $V(\mathbf{x}) \approx 40$ 

SIMP found tie-beam-like solutions when a standard continuation parameter was applied. These solutions all have inclined main beams although the coarse mesh representation artificially increased the total compliance relative to tie-beam solution in Zhou and Rozvany (2001). Thus it can be said that SIMP is less sensitive to the mesh-size since it appears to consistently find the same inclined tie-beam solution.

SIMP has many continuation paths leading to different local solutions. This was investigated by varying the initial penalisation and the initial design domain. A different continuation path was found when the rectangular initial design domain with  $P_{init} = 1.5$  was used. This new continuation path of SIMP produced a horizontal tie-beam solution which had lower compliance than the tie-beam solution in Zhou and Rozvany (2001). Therefore care is required when applying the continuation method with SIMP.

Using a fine computational mesh with SIMP gave tie-beam-like solutions with an inclined main beam when the volume constraint was specified as  $V(\mathbf{x}) \approx 40$ . These SIMP solutions using a refined mesh compared well with the ESO S-history local solutions also produced using a refined mesh with the same volume. The difference in

$S(\mathbf{x})$  was as close as 3% for some solutions, but SIMP produced the overall optimum.

When the volume constraint was specified as  $V(\mathbf{x}) \leq 99$  and a fine computational mesh was used, ESO and SIMP produced similar results, however, ESO produced the overall optimum solution.

**Acknowledgements** The authors thank Dr Lars Krog, Airbus UK, and Prof Giles Hunt, University of Bath, for their useful advice and discussion. The authors would also like to thank Prof Krister Svanberg for the MATLAB implementation of the MMA algorithm and the Numerical Analysis group at the Rutherford Appleton Lab for the FORTRAN 77 HSL package MA57. The authors acknowledge the support of UK Engineering and Physical Sciences Research Council (GR/S68477) for this research. Finally, the authors thank the anonymous referees for their inspiring and helpful comments and suggestions.

## References

- Allgower EL, Georg K (1990) Numerical Continuation Methods: An Introduction. Springer-Verlag, Berlin Heidelberg New York
- Bendsøe MP (1989) Optimal shape design as a material distribution problem. Struct Optim 1:193–202

- 
- Bendsøe MP, Sigmund O (2003) *Topology Optimization: Theory, Methods and Applications*. Springer, Berlin Heidelberg New York
- Díaz A, Sigmund O (1995) Checkerboard patterns in layout optimization. *Struct Optim* 10:40–45
- Edwards CS, Kim H, Budd CJ (2006) Investigation on the validity of topology optimisation methods. In: 47th AIAA SDM, ASC, NDA, GSF, MDO Conference, Newport, RI, USA
- Haber RB, Jog C, Bendsøe M (1996) A new approach to variable topology shape design using a constraint on perimeter. *Struct Optim* 11:1–12
- Jog CS, Haber RB (1996) Stability of finite element models for distributed-parameter optimization and topology design. *Comput Methods Appl Mech Engrg* 130:203–226
- Kim H, Querin OM, Steven GP, Xie YM (2000) A method for varying the number of cavities in an optimized topology using evolutionary structural optimization. *Struct Multidisc Optim* 19:140–147
- Martínez J (2005) A note on the theoretical convergence properties of the SIMP method. *Struct Multidisc Optim* 29:319–323
- Petersson J, Sigmund O (1998) Slope constrained topology optimization. *Int J Num Meth Eng* 41:1417–1434
- Reitz A (2001) Sufficiency of a finite exponent in SIMP (power law) methods. *Struct Multidisc Optim* 21:159–163
- Rozvany GIN, Zhou M (1991) Applications of the COC method in layout optimization. In: Eschenauer H, Mattheck C, Olhoff N (eds) *Proceedings of the International Conference on Engineering Optimization in Design Processes*, Karlsruhe, 1990, Springer Verlag, Berlin, pp 59–70
- Rozvany GIN, Zhou M, Birker T (1992) Generalized shape optimisation without homogenisation. *Struct Optim* 4:250–254
- Rutherford Appleton Laboratory (2004) *Harwell Subroutine Library*. Numerical Analysis Group, Chilton, Oxfordshire, England
- Sigmund O (1994) *Design of material structures using topology optimization*. PhD thesis, Technical University of Denmark
- Sigmund O (2001) A 99 line topology optimization code written in Matlab. *Struct Multidisc Optim* 21:120–127
- Sigmund O, Petersson J (1998) Numerical instabilities in topology optimization: A survey on procedures dealing with checkerboards, mesh-dependencies and local minima. *Struct Optim* 16:68–75
- Svanberg K (1987) The method of moving asymptotes—a new method for structural optimization. *Int J Num Meth Eng* 24:359–373
- Tanskanen P (2002) The evolutionary structural optimization method: theoretical aspects. *Comput Methods Appl Mech Engrg* 191:5485–5498
- The Math Works, Inc (2004) *MATLAB 7.0*. The Math Works, Inc., Natick, Massachusetts, USA
- Xie YM, Steven GP (1993) A simple evolutionary procedure for structural optimisation. *Computer and Structures* 49:885–896
- Xie YM, Steven GP (1997) *Evolutionary Structural Optimization*. Springer, Berlin Heidelberg New York
- Zhou M, Rozvany GIN (2001) On the validity of ESO type methods in topology optimization. *Struct Multidisc Optim* 21:80–83